ISSN: 2278 – 7798
International Journal of Science, Engineering and Technology Research (IJSETR)
Volume 6, Issue 1, January 2017

EFFECT OF SiC ON Al_2O_3-ZrB_2 COMPOSITE PREPARED BY SELF PROPAGATING HIGH TEMPERATURE SYNTHESIS (SHS)

Saravana kumar.M[1], Allen Jeffrey.J[2],Rajendra Boopathy[3],Sangeetha.D[4]
[1, 2] **Assistant Professor Department of Mechanical Engineering, Loyola Institute of Technology, Chennai**
[3, 4] **Associate Professor College of Engineering, Guindy- Anna University, India**

Abstract*— : Manufacturing process of Ceramic Matrix Composite is a challenging task now-a-days. Main objective of this project is to manufacture the ceramic matrix composite by eliminating the furnace sintering process in conventional method and introducing the self propagating high temperature synthesis (SHS). Al_2O_3-ZrB_2 ceramic matrix composite is one of the recent interests in material research. Limitation of Al_2O_3-ZrB_2 Ceramic Matrix Composite is due to its poor hardness and therefore SiC is added to improve hardness.Less expensive aluminium powder, Zirconium Oxide and Boron-Tri-Oxide were mixed in the ball mill for 3 hours to form Al_2O_3-ZrB_2 composite powder. Different weight percentages of Silicon Carbide (0%, 5% and 10%) were added to the Al_2O_3-ZrB_2 composite powder and compaction process was carried out in 10 Ton load Synthesis of green compact was carried out by self propagating high temperature synthesis (SHS) process. The formation of Al_2O_3-ZrB_2 composite was confirmed by XRD analysis. The SEM analysis confirm the homogeneity of the Al_2O_3-ZrB_2 - SiC compositeTheoretical density is compared with the theoretical density and 93.35%,93.07% and 93.75% of theoretical density has been achieved for 0wt%,5wt% and 10wt% respectively. Wear test has been conducted and influencing parameters (i.e Load, Wt% and rotational frequency) on wear loss for the prepared composite was analysed by taguchi method and it was found that addition of SiC to the Al_2O_3-ZrB_2-SiC reduces the wear loss. Hardness test for the Al_2O_3-ZrB_2-SiC Ceramic Matrix Composite has been conducted and it was found that addition of SiC to the Al_2O_3-ZrB_2-SiC improves the hardness of the composite.

***Index Terms*— SHS,Powder metallurgy,Ceramic Matrix Composite, Al_2O_3-ZrB_2**

I. INTRODUCTION

Self-propagating high temperature synthesis (SHS) is an autogenous process and derives its energy from exothermic reactions of the reactants. Now a day's SHS has recently been used extensively for preparing refractory materials such as carbides, silicides, nitrides, and various composite materials. The synthesis is initiated by point heating of a small part of the sample. Once started, a wave of exothermic reaction sweeps through the remaining material

It is energy efficient and fast process compared to the conventional processes such as solid state reaction, and carbothermal reactions. Normally conventional processes require very high temperature processing and multi-steps such as calcinations, grinding in between, and pelletisation. Sintering along with hipping is normally required for better dense materials. However SHS does not need many of these steps during synthesis and sintering. Often in composite fabrication, the powders have been made by SHS process and then sintered at higher temperatures. Multiple processing steps make the process time consuming. Though higher densities have been achieved during furnace sintering, the large grain growth degrades the mechanical properties of the composite. Another way is to use an economical process, which not only synthesize but also dandifies the composite in-situ in SHS dynamic compaction. SHS dynamic compaction is energy efficient, fast process and can be used for simultaneous densification during the SHS reaction to form the in situ composite. Here loads are applied during the SHS reaction to density the SHS reaction product. Often dynamic compactions are done with metallic powder, but few reports show the use of oxides during SHS propagation and simultaneous densification of the product. SHS dynamic compaction is an attractive process, where proper control of the SHS processing parameters such as time of pressing, interval of loading and load applied during the process is very critical to yield a fully dense product. Improper synthesis time, loading time and load lead to cracked and porous materials. Metallic binders and diluents are often used to control the SHS process. Metallic binder, which has the lower melting temperatures, melts during the reaction leading to change in rate of reaction and hence better densification. Besides the metallic diluents, similar powders are also used as diluents to control the SHS reaction. These diluents not only give higher densification but also inhibit grain growth. The incorporation of high temperature boride particulates improves the properties of ceramic matrix composites in terms of mechanical strength, abrasion & wear of the composite.

S.K. Mishra et. Al (2014), fabricated an Alumina–Zirconium diboride in situ composite with different Ti percentages as diluents during SHS reaction. It was observed that Ti addition leads to the formation of different phases such as TiB_2, ZrO_2, TiB along with ZrB_2 and Al_2O_3 which were not found when Titanium was not added, it had only Al_2O_3 and ZrB_2. With an increase of Ti content eutectic phase of ZrO_2 and Al_2O_3 was also observed in the

microstructure. The hardness was found to be a maximum of 2150 HV0.1 for 5 wt.% Ti diluents, further it decreased with the addition of Ti. However the depth indentation showed maximum for 10 wt.% Ti addition. The hardness and modulus were found to be around 21 GPa and 350 GPa, respectively for 10 wt.% Ti addition. **C.L. Yeh et. Al (2006)** investigated the preparation of TiAl intermetallic compounds with or without the reinforcement phase TiB_2 was conducted by self-propagating high temperature synthesis (SHS) from elemental powder compacts in this study. Effects of initial sample density, preheating temperature, particle size of the reactants, and TiB_2 content on the combustion characteristics, as well as on the composition and morphology of final products were studied. In this investigation, preheating was found to be required for the samples without boron addition to achieve self-sustained combustion, while boron-added compacts showed no need of prior heating, primarily due to the additional reaction heat liberated from the in situ formation of TiB_2. With the addition of boron, the reaction temperature and flame-front propagation velocity were correspondingly increased. Due to the melting of synthesized products caused by high-combustion temperatures, the TiAl–TiB_2 composite was contracted in dimension during the reaction. On the contrary, substantial volume expansion was observed in the sample without boron addition. This means that the in situ formed TiB2 plays an important role not only in improving the mechanical property, but also in enhancing the densification of final products. XRD analysis of burned products identifies the in situ formed TiB2 a reinforcing phase, and TiAl the dominant intermetallic phase. In addition to TiAl, another intermetallic compound Ti_3Al known as a major secondary phase in the Ti–Al reaction was detected in all end products of this study.**S.K. Mishra et. Al (2014),** fabricated an Alumina–Zirconium diboride in situ composite with different Ti percentages as diluents during SHS reaction. It was observed that Ti addition leads to the formation of different phases such as TiB_2, ZrO_2, TiB along with ZrB_2 and Al_2O_3 which were not found when Titanium was not added, it had only Al_2O_3 and ZrB_2. With an increase of Ti content eutectic phase of ZrO_2 and Al_2O_3 was also observed in the microstructure. The hardness was found to be a maximum of 2150 HV0.1 for 5 wt.% Ti diluents, further it decreased with the addition of Ti. However the depth indentation showed maximum for 10 wt.% Ti addition. The hardness and modulus were found to be around 21 GPa and 350 GPa, respectively for 10 wt.% Ti addition. This is due to the fact that nano indentation hardness and modulus are dynamic hardness and depend on elastic plastic behaviour of the composite where as in case of micro hardness it is static hardness. It is due to the fact that borides at the upper surface of the composite oxidise which further inhibit the penetration of oxygen so the plateau region is observed. However the weight change was very minimal and no significant change was observed after 700 °C oxidation in terms of phase, hardness and modulus values. Hence they are stable under oxygen at 700 °C. The toughness of 20 wt% Ti sample had very high fracture toughness 45 MPa m−1/2; considering the fact that fracture toughness of ceramics on average is quiet low. The Kc values were 18.25, 15.43, and 29.6 MPa m−1/2 for 5, 10 and 25% Ti addition, respectively. Composite with no Titanium did not show any crack even at 20 kgf force under indentation. The initial sliding wear studies with WC ball showed very less wear under the experimental condition of the experiment

II. MATERIAL AND METHOD

A. *Experimental work:*

Ball Milling of Ingredients:

Raw materials were mixed in the Ball Mill for 3 hours. Table 1 shows the various wt% of the SiC in the Al2O3-ZrB2 composite.

Table 1. Wt% of the SiC on Al_2O_3-ZrB_2 composite

Specimens	**Wt%**			**Wt % of SiC**	**BPR(Ball to Powder Ratio)**
	Al	ZrO_2	B_2O_3		
Specimen 1	62.5	18.75	18.75	0	23:1
Specimen 2	62.5	18.75	18.75	5	23:1
Specimen 3	62.5	18.75	18.75	10	23:1

B. *Fabrication of Die*

Upper Half of the Die

The figure 1 illustrates the upper half of the chamber. The initial material Hot-rolled steel (H11 grade) procured for the upper half is 56 mm diameter. Turning on the outer surface was done to reduce diameter to 55 mm. This was followed for the first 25 mm and the rest was machined to 49.94 mm in order to snugly fit the interface. Initially turning was carried out followed by coarse grinding and then fine grinding leading to 49.94 mm. followed. This gives a tight pressure set-up after adhesive bonding.

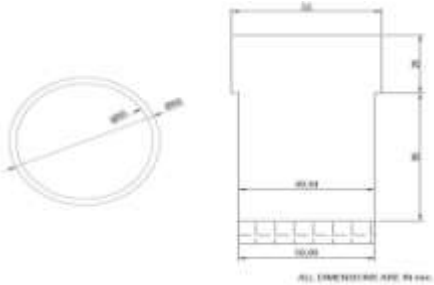

Figure 1. Line diagram of upper half of die

Lower Half of the Die

The figure 2 illustrates the lower half of the die. The same material procured was 110 mm dia and then turned to 100 mm diameter. A bore of 50 mm was made using lathe. Two holes were then drilled using copper wire based erosion spark drilling otherwise known as electric discharge machining (EDM) leading to 1mm diameter holes so that the pressure inside the chamber is maintained.

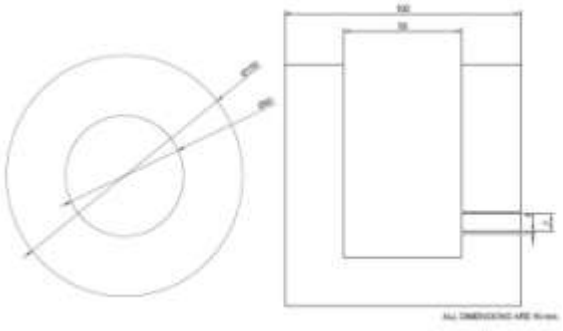

Figure 2. Line diagram of lower half of die

Heat Treatment of Chamber

The finishing operations of the material were carried out and then turned and faced to the required dimension. Heat

treatment was then carried out by hardening at 1010 ^{0}C for 2 hours followed by air quenching to room temperature. This was then medium temperature tempered at 510°C for 1 hour. The final hardness observed was 48 HRC. The heat treatment cycle is shown in figure 3

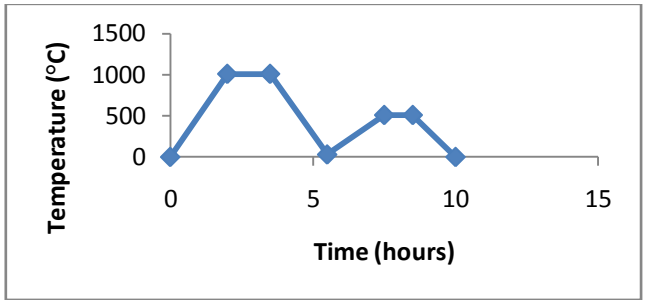

Figure. 3 Heat Treatment Cycle

The heat treated steel was then coarse ground using Silicon Carbide Grinding Wheel. The die was then drilled with 1 mm drill using erosion spark drilling or electric discharge machining. The figure 4 shows the upper and lower part of the die after heat treatment and finishing operations.

Figure 4 Fabricated die

Fabrication of composite by cold pressing and SHS process

The mixture was pelletised in the cylindrical form of 50 mm diameter and 10 mm length. The pelletisation was carried out at 10 ton load. The SHS reaction and dynamic compaction processing's were carried out in an air atmosphere, in a die made of die steel. The reaction of the pellets was ignited with an electrically heated tungsten coil placed at the side surface of the green pellets. When the reaction started, the ignition source was switched off. The reactions were carried out for synthesis times (T_s), 6 s, with loading times, called as delay time (T_d) 3 s. When Ts was reached a pressure of 5MPa was applied. The following reaction takes place during Self Propagating High Temperature Synthesis process.

$$3ZrO_2 + 3\,B_2O_3 + 10\,Al \rightarrow 3ZrB_2 + 5Al_2O_3$$

C. Characterization of Composite

X – Ray Diffraction (XRD)

To confirm the formation of Al_2O_3-ZrB_2 , X-Ray diffraction analysis is conducted. Prepared composite is crushed into powder is analyzed and studied using the room temperature powder X-ray diffraction (Analytical X'Pert Pro Powder XRD system) with filtered 0.154056 nm Cu Kα radiation. Samples are scanned in a continuous mode from 20° – 90° with a scanning rate of 0.02 (degree) / 1 (sec).The results of the X-Ray diffraction analysis and the particle size are discussed in the results and discussion

Scanning Electron Microscopy

The micro structural features and morphology of the fabricated specimens were analyzed using a Scanning Electron Microscope (HITACHI-S3400N).The image was take at magnification of 250X. Data size 1280 x960 and pixel size 396.875points was maintained.

Peak no.	2 θ	θ	$Sin^2\theta$	($sin^2\theta/sin^2\theta_{min}$)	K factor	$h^2+k^2+l^2$	(h,k,l)
1	28.519	14.259	0.0606	1.0000	3	3	(1 1 1)
2	31.82	15.936	0.0753	1.2425	3.7275	4	(2 0 0)
3	38.876	19.438	0.1107	1.8267	5.4801	6	(2 1 1)
4	45.115	22.550	0.1470	2.4257	7.2771	8	(2 2 1)
5	65.464	32.732	0.2923	4.8234	14.101	14	(3 2 1)
6	78.572	39.286	0.4009	6.6155	19.8465	20	(4 2 0)

Pre-processing of specimens for SEM

Successively finer abrasive particles(Silicon Carbide) are used to remove material from the sample surface until the desired surface quality is achieved after grinding process polishing is done by slurry of alumina and quarter portion of the each samples were taken out, subsequently the samples were etched using etchants called nital and placed in the mould and the mould is introduced into the scanning electron microscope Figure 5 shows the specimens in which one portion is taken out and the figure 6 shows the specimen placed in the mould to be subjected to the scanning electron microscopy to analyze Al_2O_3-ZrB_2-Sic composite

.

Figure 5 SEM Specimens taken out from the final product

Figure 6. SEM Specimen placed in the mold

D. Testing of Properties of the Composite

Density of the prepared Composite

Theoretical density of the composite been calculated by the concept of rule of mixture which is explained inresults and discussion. Actual density of the composite is computed by Archimedes principle. For Archimedes principle, first each specimen were measured in the air and noted as m_1.water of 500ml is taken in the beaker and the first specimen whose density to be calculated is immersed in the water and reading were noted as m_2 from the electronic weighing scale. Now the density of the specimen is calculated fro the following equation.

$$m_1-m_2 = \rho.v .g \ldots\ldots\ldots(1)$$

Wear Test

Two-body abrasive wear tests were conducted on a pin-on-drum abrasive wear tester, designed for standard wear tests described in ASTM Standard D5963-97a. In this method, the test specimen translates over the surface of an abrasive paper, which is mounted on a revolving drum, with the resulting wear of the material expressed as mass loss . An alumina (Al2O3) abrasive which is substantially harder than either the matrix or the reinforcement was used. The pin specimen, 0.95 mm in diameter and 20 mm long, was placed on the top of the drum, which was then rotated at a fixed angular speed of 40±1RPM . A static normal load, 1kg i.e 9.81 N, was applied directly on the specimen to press it against the center of the drum. Throughout the test, the sliding distance was fixed at 39.2 m (84 revolutions). All tests were carried out in dry ambient air condition

Hardness test

D5873 - 14 *Standard* Test Method for Determination of Rock well Hardness is followed. Specimen of 50mm diameter and 15mm thickness and conical diamond with a round tip of 1/8" is used as ball indenter.100kgf load been applid and the reading were taken in the B-Scale.

III. Results and Discussion

A. Final Product

Figure 7 shows the final product of the specimenprepared through self propagating high temperature synthesis process and it was observed that synthesis took place uniformly throughout in all the three (0wt%,5wt% and 10wt%) specimens.

Dimension of the final product was measured to be 50mm in diameter and 10mm in length

Figure 7 Final Product of the Composite Prepared

B. X-Ray diffraction analysis

Plotting of graph using Origin-pro 8 Software

Data obtained from XRD analysis is plotted as a graph using Origin-pro 8. Intensity in counts was taken in Y axis and angle of diffraction was taken in X axis and Fig 8 shows the centre points of the peak and corresponding graph drawn in the Origin pro 8 software. There are totally 6 peaks are found and their centre point (i.e. the maximum intensity) is predicted. Table 2 shows the calculation of (h, k ,l) (Miller indices

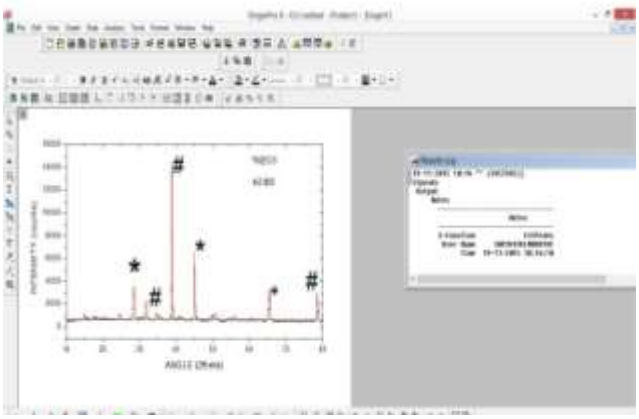

Figure 8. Plotting of graph in Originpro 8

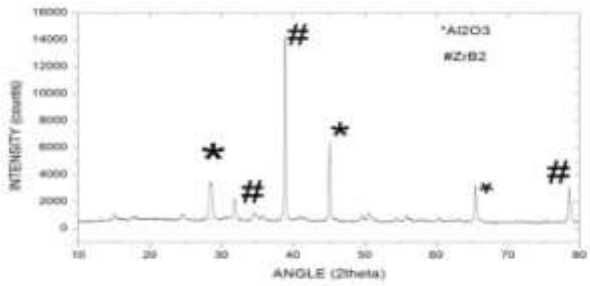

Fiureg 9 XRD pattern of the Specimen

From the figure 9 ,it is observed that the plot drawn in the origin –pro 8 is match with the JCPDS file and therefore the formation of Al_2O_3-ZrB_2 is confirmed

c. Sem analysis

Figure 10 (a,b,c) shows the 2500X Scanning Electron Microscope image of Al_2O_3-ZrB_2 Ceramic Matrix Composite with varying weight percentage (0, 5, &10) of SiC. The shape of the synthesized specimens is uniform. SiC is uniformly distributed throughout the specimens in all the three cases

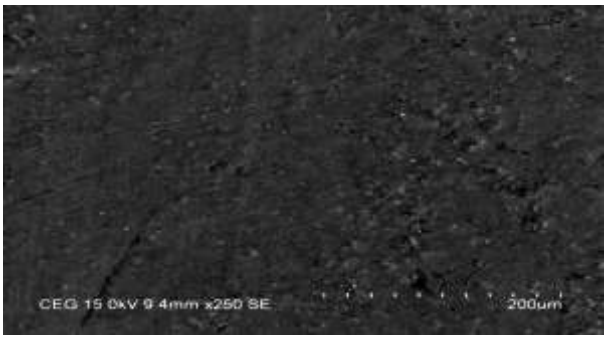

0wt% of Sic

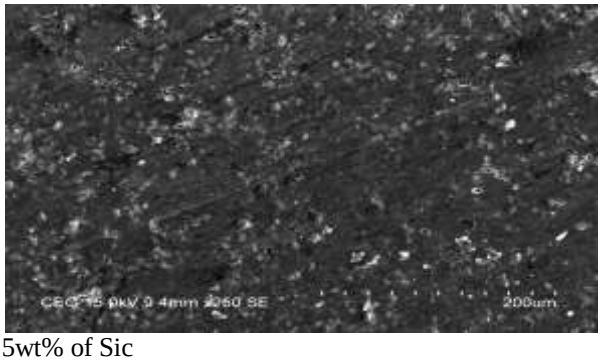

5wt% of Sic

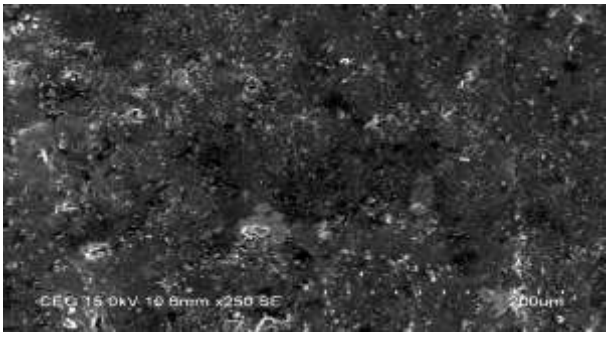

10wt% of Sic

Figure.10 SEM images of specimen

D. Density of the prepared Composite:

Theoretical density of the specimen were calculated by the concept of Rule of Mixture and the actual density of the composite is calculated by Archimedes principle. From the graph (figure. 11&12) it is concluded that adding of soft reinforcement i.e Silicon carbide (SiC) to the hard matrix reduces the density of the composite

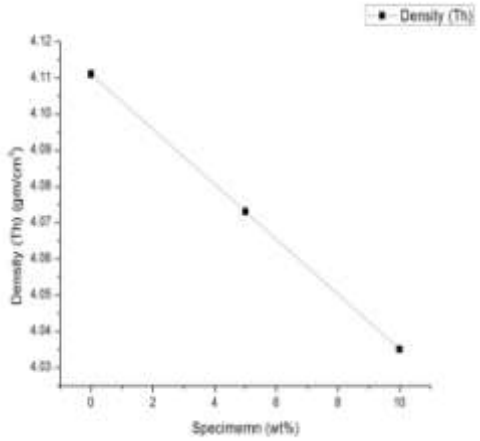

Figure. 11 Graph fot theoretical density versus wt%

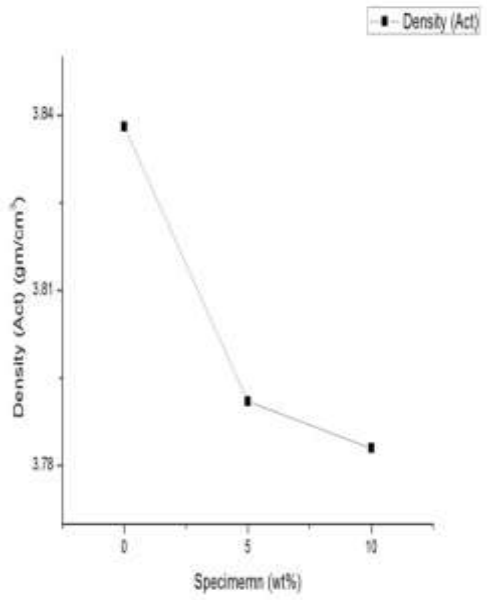

Figure.12 Graph for Actual density versus Wt%

D. Comparision of Actual density With Theoretical Density

Table 3 and the figure 13 shows the comparison between the actual density and theoretical density. 93.35%,93.07% and 93.75% of theoretical density has been achieved for 0wt%,5wt% and 10wt% respectively

Table 3 Comparision of Actual density With Theoretical Density

Specimen (wt% of SiC)	Theoretical Density (gm/cm^3)	Actual Density(gm/cm^3)
0	4.111	3.838
5	4.073	3.791
10	4.035	3.783

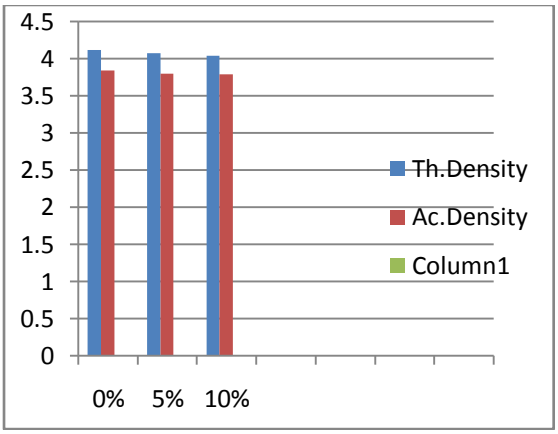

Figure.13 Bar chart for Theoretical Density versus Actual Density

E.Calculation for Porosity

Porosity of eah specimen was calculated by using the following formula.

$$porosity = \frac{Theortical\ \ density\ -Actual\ \ density}{Theortical\ \ density} \times 100$$

Table 4 and figure 14 shows the porosity present in the each specimen.

Table 4 Porosity for the prepared composite

Speimens (Wt%)	**Porosity (%)**
0	**6.64**
5	**6.923**
10	**6.24**

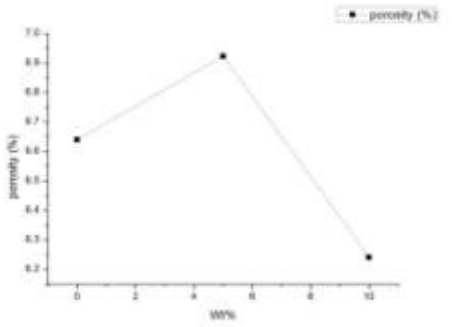

Figure 14 Graph for porosity vs wt %

F. Wear Test:

Two-body abrasive wear tests were conducted on a pin-on-drum abrasive wear tester, designed for standard wear tests described in ASTM Standard D5963-97a. Wt%,Load and Rotational frequency are analysed as a factor at various level listed in the table 5 by Taguchi method.

Table 5 Factors at various level

Level / Factor	1	2	3
Wt(%)	0	5	10
Load (N)	9.810	14.715	19.620
Rotational Frequency (r.p.m)	40	45	50

As there are 3 factors (Wt%, Load and Rotational frequency) at 3 levels are analysed, (L_9) Orthogonal Array was chosen . Table 4.5 shows the (L_9) Orthogonal Array and the runs of the experiment at various levels. Based up on these runs abrasive wear of the each specimen is observed and amount of material removed in grams is notes as abrasion loss which is listed in the table 7

Table 6 Orthogonal Array (L_9)

Wt %	Load (N)	Rotational frequency(rpm)
0	9.810	40
0	14.715	45
0	19.620	50
5	9.810	45
5	14.715	50
5	19.620	40
10	9.810	50
10	14.715	40
10	19.620	45

Table 7 Orthogonal Array (L_9) With Response (Abrasion Loss)

Wt %	Load (N)	Rotational frequency(rpm)	Initial Weight (gm)	Final Weight (gm)	Abrasion Loss (gm)
0	9.810	40	4.8442	3.8986	0.9456
0	14.715	45	4.8442	3.8263	1.0179
0	19.620	50	4.8442	3.7380	1.1062
5	9.810	45	4.4907	3.5880	0.9027
5	14.715	50	4.4907	3.4380	1.0527
5	19.620	40	4.4907	3.6691	0.8216
10	9.810	50	4.1199	3.3880	0.7319
10	14.715	40	4.1199	3.4501	0.6698
10	19.620	45	4.1199	3.4310	0.6889

Table 8 shows the Analysis of variance (ANOVA) for the abrasion loss of the prepared Al_2O_3-ZrB_2-SiC .From the ANOVA table we can conclude that for Wt% calculated F value (60.63) is higher than the tabulated value (at α=0.5 and υ at (2,2) is 19.33) which means that weight percentage of each specimen is to be taken in to consideration as more influencing factor on the abrasion loss.For other factors, Load and rotational frequency,the calculate F value is less than the tabulated value.

Table 8 ANOVA for Wear

Source	Degree of freedom	Sum of Square	Mean Sum of Square	F	P	Remarks
Wt %	2	0.168384	0.084192	60.63	0.016	Significant
Load (N)	2	0.004700	0.002350	1.69	0.371	Insignificant
Rotational frequency (rpm	2	0.034980	0.034980	12.60	0.074	Insignificant
Residual Error	2	0.002777	0.002777			
Total	8	0.210841				

Table 9 shows the taguchi rank for the factors based up on their influence on abrasive loss. As already stated that Wt% of the specimen plays major role on abrasion loss which gets rank 1 and next to Wt% Load (N) and rotational frequency are in rank 2 and 3 respectively

Table 9 Response Table for Wear

Level	Wt %	Load (N)	Rotational frequency(rpm)
1	1.0232	0.8601	0.8123
2	0.9257	0.9135	0.8698
3	0.6969	0.8722	0.9636
Delta	0.3264	0.0534	0.1513
Rank	1	3	2

Same Anova table and response table for abrassion loss been verified using Minitab (version 16) software and main effect plot for means were obtained which is shown in figure 15,16 and in 17

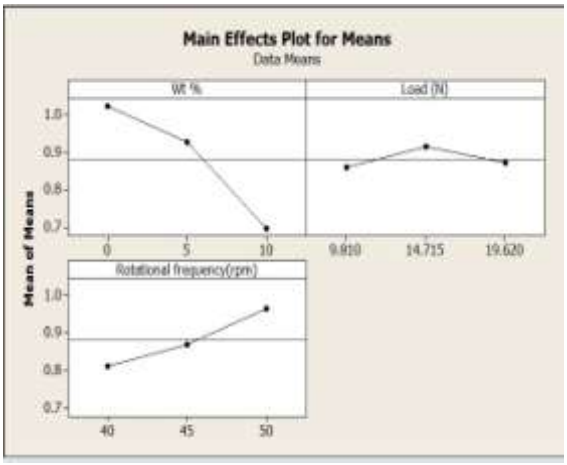

Figure 15 Main Effect Plot for Means

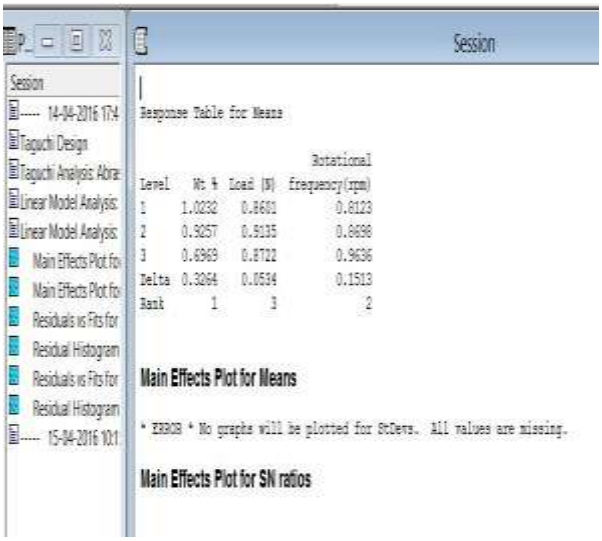

Figure 16 Response table in Minitab

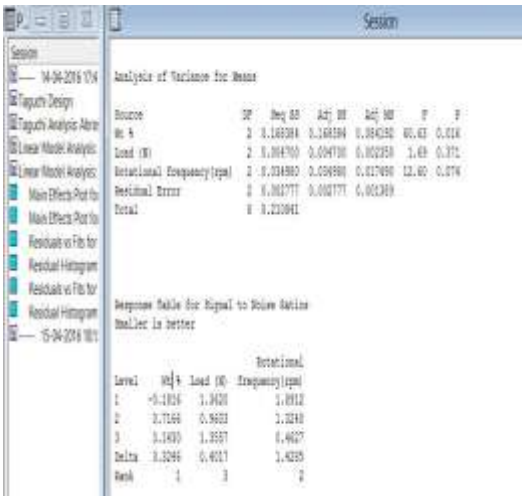

Figure 17. ANOVA in Minitab (version 16)

Regression equation for wear
The regression equation is,

Abrasion Loss (gm) = 0.346 - 0.0326 Wt % + 0.00124 Load (N) + 0.0151 Rotational frequency(rpm)
Interpretation from Regression equation:

Predictor	Coef	SE Coef	T	P
Constant	0.3462	0.2247	1.54	0.184
Wt %	-0.032637	0.004694	-6.95	0.001
Load (N)	0.001240	0.004785	0.26	0.806
Rotational Frequency(rpm)	0.015127	0.004694	3.22	0.023

As p value for wt% and load are less than the α value (0.05) we can say that Wt% and load plays more significant factor on abrasion loss, on other hand rotation frequency (r.p.m) has no significant effect on abrasion loss.

.

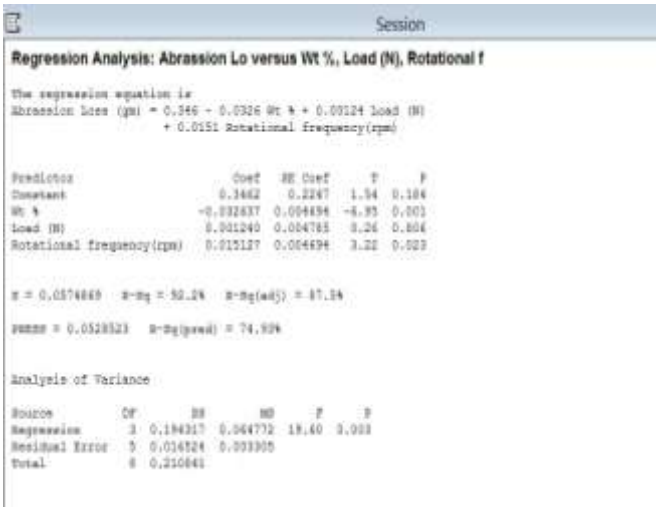

Figure 18 Regression equation in the Minitab 16

F.Hardness Test

D5873 - 14 Standard Test Method for Determination of Rock well Hardness is followed. Specimen of 50mm diameter and 15mm thickness and conical diamond with a round tip of 1/8" is used as ball indenter.100kgf load been applid and the reading were taken in the B-Scale which is tabulated in table 10

Table 10 Rockwell Harness B scale Readings

Sl .No	Specimen	Hardness (HRB)			
		Trial 1	Trial 2	Trial 3	Mean
1	0%	B36	B35	B37	B36
2	5%	B44	B36	B44	B41
3	10%	B46	B48	B50	B48

Regression Equation for Hardness

The regression equation is,

Hardness = 35.7 + 1.20 wt%

Fig.19 shows the Regression analysis for Hardness in Minitab software.

```
Welcome to Minitab, press F1 for help.

Regression Analysis: Hardness versus wt%

The regression equation is
Hardness = 35.7 + 1.20 wt%


Predictor     Coef  SE Coef      T      P
Constant   35.6667   0.7454  47.85  0.013
wt%         1.2000   0.1155  10.39  0.061


S = 0.816497   R-Sq = 99.1%   R-Sq(adj) = 98.2%

PRESS = 9   R-Sq(pred) = 87.61%


Analysis of Variance

Source          DF      SS      MS       F      P
Regression       1  72.000  72.000  108.00  0.061
Residual Error   1   0.667   0.667
```

Fig.19 Regression for Hardness in Minitab 16

G.Interpretation from Regression Equation:

As Adjusted R^2 value is 98.2% the generated regression equation if exactly fit for the given input (i.e by Wt%) That means 98.2% of hardness is determined by %SiC.

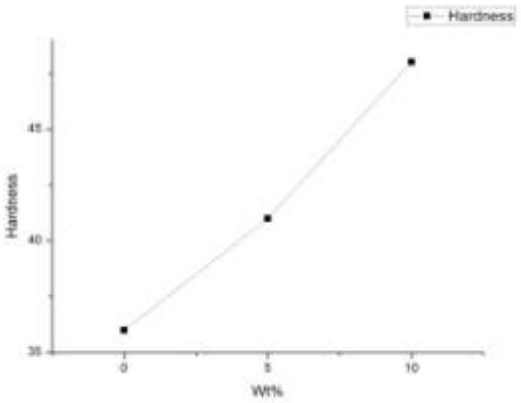

Figure 20 Wt% versus Hardness

From the figure 20 we can conclude that adding of SiC to the prepared Al_2O_3-ZrB_2 is improving the hardness.

IV. CONCLUSSION

1. An inexpensive and efficient set up for SHS was designed and developed.
2. Al_2O_3-ZrB_2-SiC Ceramic matrix composite was prepared using the designed apparatus.
3. Phase analysis using XRD was performed to confirm the formed Al_2O_3-ZrB_2.
4. SEM analysis were used to analyze the Al_2O_3-ZrB_2-SiC with various percentage of SiC .
5. Theoretical density is compared with the theoretical density and 93.35%,93.07% and 93.75% of theoretical density has been achieved for 0wt%,5wt% and 10wt% respectively
6. Porosity in the prepared composite is analysed and found presence of porosity is minimum
7. Wear test has been conducted and influencing parameters (i.e Load, Wt% and rotational frequency) on wear loss for the prepared composite was analysed by taguchi method and it was found that addition of SiC to the Al_2O_3-ZrB_2-SiC reduces the wear loss
8. Hardness test for the Al_2O_3-ZrB_2-SiC Ceramic Matrix Composite has been conducted and it was found that addition of SiC to the Al_2O_3-ZrB_2-SiC improves the hardness of the composite

REFERENCES:

1. Roberta Licheri, Roberto Orrù , Clara Musa, Giacomo Cao (2007) “Combination of SHS and SPS Techniques for fabrication of fully dense ZrB2-ZrC-SiC composites” Materials Letters 62 (2008) 432–435.

2. C.L. Yeh, S.H. Su (2005) “In situ formation of TiAl–TiB2 composite by SHS” Journal of Alloys and Compounds 407 (2006) 150–156.

3. F.L. Zhang, Z.F. Yang, Y.M. Zhou, C.Y. Wang, H.P. Huang (2011)“Fabrication of grinding tool material by the SHS of Ni–Al/diamond/dilute” Int. Journal of Refractory Metals and Hard Materials 29 (2011) 344–350.

4. S.K. Mishra, Khusboo, V.A. Sherbakov (2011) “Fabrication of in-situ Ti–Si–C fine grained composite by the self propagating high temperature synthesis (SHS) process” Int. Journal of Refractory Metals and Hard Materials 29 (2011) 209–213.

5. S.K. Mishra, Khusboo, V.A. Sherbakov (2007) “Fabrication of Al2O3–ZrB2 in situ composite by SHS dynamic compaction: A novel approach” Composites Science and Technology 67 (2007) 2447–2453

6. S.K. Mishra, A. Bhople, S. Paswan (2014) “Microstructure, hardness, toughness and oxidation resistance of Al2O3–ZrB2 composite with different

Ti percentages prepared by in-situ SHS dynamic compaction" Int. Journal of Refractory Metals and Hard Materials 43 (2014) 7–12.

7. Takeshi Tsuchida, Satoshi Yamamoto (2003) "MA-SHS and SPS of ZrB2–ZrC composites" Solid State Ionics 172 (2004) 215–216

8. E. Taheri-Nassaj, S.H. Mirhosseini (2003) "An in situ WC–Ni composite fabricated by the SHS method" Journal of Materials Processing Technology 142 (2003) 422–426.

9. Takeshi Tsuchida, Tsuyoshi Kakuta (2005) "Synthesis of NbC and NbB2 by MA-SHS in air process" Journal of Alloys and Compounds 398 (2005) 67–73.

10. P. Istomin, A. Nadutkin, V. Grass (2012) "Fabrication ofTi3SiC2-based ceramic matrix composites by a powder-free SHS technique" Ceramics International 39 (2013) 3663–3667.

11. Xuanyi Yuan, Guanghua Liu, Haibo Jin, Kexin Chen (2011) "In situ synthesis of TiC reinforced metal matrix composite (MMC) coating by self propagating high temperature synthesis (SHS)" Journal of Alloys and Compounds 509 (2011) L301– L303.

12. Manoj Masanta , P. Ganesh, Rakesh Kaul , A. Roy Choudhury (2010) "Microstructure and mechanical properties of TiB2–TiC–Al2O3–SiC composite coatings developed by combined SHS, sol–gel and laser technology." Surface & Coatings Technology 204 (2010) 3471–3480.

13. Fang Wen,Tao Lin, Xiangqing Liu (2012) "Effects of microstructure characterization of SHS TiC reinforced Fe composite coating." Procedia Engineering 27 (2012) 1738 – 1743.

14. M. Sakaki, A. Karimzadeh Behnami, M.Sh. Bafghi(2014) "An investigation of the fabrication of tungsten carbide–alumina composite powder from WO3, Al and C reactants through microwave-assisted SHS process." Int. Journal of Refractory Metals and Hard Materials 44 (2014) 142–147.